

Optical studies of the magnetic phase diagram of FeCl_2

J. F. Dillon, Jr., E. Yi Chen, and H. J. Guggenheim

Bell Laboratories, Murray Hill, New Jersey 07974

(Received 6 July 1977)

The magnetic phase diagram of FeCl_2 in fields along [0001] has been determined anew with greater accuracy using magneto-optical-rotation and light-scattering techniques. The Néel point and the tricritical point have been found to be 23.7 and 21.60 K, respectively. In the rotation-temperature plane the phase boundaries approach the tricritical point nearly linearly. A careful comparison of these data with those of Griffin *et al.* and those of Birgeneau *et al.* leads to the conclusion that all three are in essential agreement near the tricritical point, a result consistent with tricritical theory.

I. INTRODUCTION

In this paper, we present the results of optical measurements of the magnetic phase diagram of the metamagnetic crystal FeCl_2 with particular emphasis on the neighborhood of the tricritical point (TCP). Both magneto-optical-rotation and light-scattering techniques have been used.

FeCl_2 is a particularly attractive system in which to make a detailed study of tricritical phenomena. It exemplifies a class of Ising-like antiferromagnets in which the spin sublattices are alternating layers. There has been a large body of work on the magnetic properties of the compound and many of its properties are known and well understood.¹ It is a good starting material for possible studies of cooperative magnetic phenomena in mixed systems, either anions or cations may be diluted. In earlier work, we found that FeCl_2 exhibits large magneto-optical effects and that these offered the possibility of studying the tricritical diagrams with more accuracy than has been done previously. The details of these phase diagrams have a special interest at this time because of the important prediction of modern theory² that the approaches to the tricritical point are very similar to those expected on the basis of Landau-type theory. Results on He^3 - He^4 mixtures support this.³ Recent results on a metamagnet with interpenetrating sublattices (dysprosium aluminum garnet in fields along [110]) also showed approaches of the first-order phase lines to the tricritical point on the M - T phase diagram as in Landau theory.⁴ However, for the layer-structure archetype FeCl_2 the experimental situation has been singularly unclear. Two earlier sets of measurements, one using neutron diffraction,⁵ the other magnetic circular dichroism⁶ yielded tricritical phase diagrams which differed substantially. The two determinations agreed in finding almost linear approaches of the paramagnetic line and the λ line

to the tricritical point. The experiments using magnetic circular dichroism (MCD) found the approach to the TCP along the antiferromagnetic line to be roughly linear in accord with the theoretical prediction. In contrast the neutron-diffraction results showed a sharply curving approach. Though further details and definitions will be given later, the two reported values for β_c were 1.13 ± 0.14 and 0.36. There were also significant discrepancies in the values of T_t , T_N , and T_t/T_N in the two reports.

This work was undertaken to determine the tricritical phase diagram of FeCl_2 with greatly increased accuracy. This was to be done using magneto-optical techniques. Further, it was hoped that the results would resolve the discrepancy between the earlier determinations.

For our present purposes the structure of FeCl_2 consists of hexagonal sheets of $S=1$ Ising spins within which spins are coupled ferromagnetically. A considerably smaller antiferromagnetic coupling is operative between the sheets. The layer nature of the structure dominates the mechanical properties. The crystals are soft and peel easily.

As background we show schematically in Fig. 1 magnetic phase diagrams of FeCl_2 as presently understood. Our experiments are aimed at quantifying these sketches. In FeCl_2 at low temperatures and fields along the c axis, the spins in a layer of Fe^{2+} ions all lie parallel to each other and normal to the layer. The spins in the two adjacent layers are antiparallel. The H_1 - T phase diagram is schematized in Fig.1(a). At zero field this antiferromagnetic state persists up to the Néel point T_N . Beginning at 0 K there is a specific value $H_c(T)$ of internal field for which there is a first-order transition to a paramagnetic state in which the spins are aligned and two sublattices are no longer distinguishable. This antiferromagnetic to paramagnetic transition is first order up to a tricritical point where, according to classical theory, the first-order line joins smoothly on

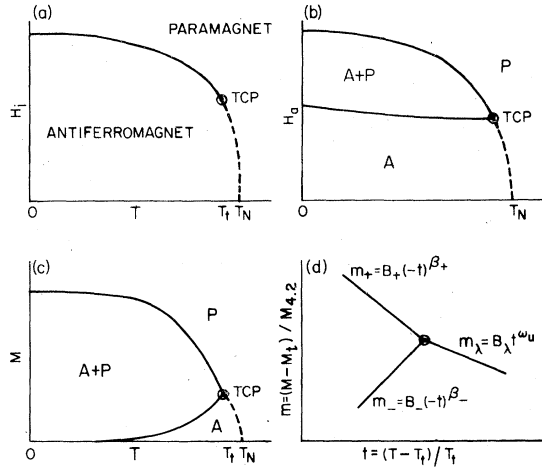


FIG. 1. Sketches of the phase diagrams of FeCl_2 as presently understood. (a) the H_z - T plane, (b) the H_a - T plane, (c) the M - T plane, and (d) sketch adapted from Ref. 7 illustrating the definitions of the exponents used to describe the approach of the phase transitions to the tricritical point in a reduced M versus a reduced T plane. Note a slight change from Ref. 7 in that we use $M_{4,2}$ to reduce that magnetization rather than M_t . Later it will be seen that we use parallel definitions based on rotation for these same exponents.

to a second-order line. This λ line goes to T_N , and the whole structure is reflected into negative field.

Demagnetizing effects open the coexistence line into a coexistence area for the corresponding plot in H_a - T as shown in Fig. 1(b). Within the area marked $A+P$ the two states coexist in varying proportions. In Fig. 1(c) is sketched the phase diagram in the M - T plane. Here the magnetizations of the two phases along the coexistence line diverge rapidly on leaving the tricritical points. The convention we will use for describing the curvature in the region around the tricritical points is shown in Fig. 1(d). The sketch follows Wolf.⁷ Exponents β_+ and β_- pertain to the paramagnetic and antiferromagnetic branches, and ω_u describes the approach of the critical line.

II. SAMPLES AND APPARATUS

The rotation and scattering measurements reported here require that a thin sheet sample be immersed in a magnetic field normal to its major faces, that its temperature be measured and controlled, and that it transmit a beam of polarized light. With the drawing in Fig. 2 we describe these arrangements briefly.

The phase diagram data quoted here all pertain to a single sample of FeCl_2 , though less extensive experiments on four other specimens were com-

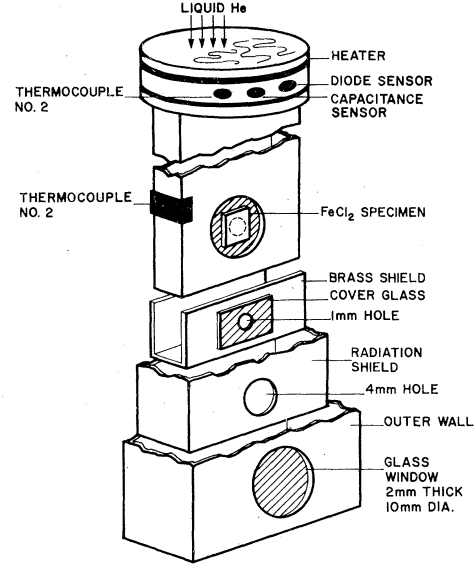


FIG. 2. Sketch of the sample mounted on a thermostatted copper rod within the temperature shields of a variable temperature Dewar.

pletely consistent. This was a nearly square piece $4 \times 4 \times 0.075$ mm cut from a sublimation flake. The preparation technique was described in Ref. 8.

The sample was mounted on a copper bar extending down from the cold block of a variable temperature Dewar.⁹ This was positioned so that the sample was on the axis of a 12-in. electromagnet whose pole pieces had been drilled for optical access. As sketched in Fig. 2, the crystal is set in a recess in the copper bar, over a small hole. Around the edges it is embedded in high thermal conductivity grease. The small central region through which light passes is exposed to the vacuum. A folded brass sheet slips over the end of the bar to shield the sample from unnecessary thermal radiation. The 1-mm holes in this shield are covered with cover glasses. The steep slope in the field width of the $A+P$ region in the 18- to 20-K range was used to demonstrate that for the final configuration thermal radiation and the measuring radiation did not raise the sample temperature significantly. With the block held at one temperature, a trace of scattering intensity versus field gives a very good measure of the width of the mixed phase region, as discussed later. As the size of the holes in the brass shield was reduced this width at first increased as the sample temperature became lower. Reduction of the hole size beyond a certain size or introduction of the cover glass had no further effect. Thus, the shield and the cover glass had eliminated spurious heating of the sample by radiation, and its temperature was surely that of the block by which it is almost

completely surrounded.

The copper block is shielded from room-temperature radiation by a radiation shield maintained at about 20 K. Outside of this the outer wall of the Dewar is fitted with optically flat windows of glass. The interconnected space between the rod and the radiation shield and the outer wall is evacuated. The sample is several inches below the block whose temperature the Dewar controls. This is cooled by a slow flow of liquid helium brought to it by a liquid-helium cooled transfer tube.⁹ It is warmed by a heater coil. Its temperature is sensed by a calibrated silicon diode whose calibration is only valid in zero field. There are two gold (0.07-at. % Fe)-chromel thermocouples, one on the block, one on the bar very close to the sample. From these we know that except when the temperature is changing, there is no measurable difference between the two couples. The capacitance sensor which is not field sensitive is used in conjunction with a controller¹⁰ to thermostat the block. At the temperatures of greatest interest the controller gives stability of ± 0.01 K over the five or ten minutes necessary for a rotation versus field plot.

III. MAGNETO-OPTICAL ROTATION

The central measurements in this work are of the magneto-optical rotation of linearly polarized light on passage through thin (0001) sheets of FeCl_2 with magnetic field and propagation direction along [0001]. These have been made as field, temperature, and wavelength varied. Rotation is an attractive quantity on which to concentrate. For many purposes it may be regarded as an order parameter itself. It is very closely proportional to magnetization and thus can be used to determine demagnetizing effects. From an experimental point of view, rotation measurements have the advantage that they can be made rapidly with great accuracy. Only optical access to the specimen is required. Although it is impractical to make ellipsoidal specimens of soft layer structure crystals such as FeCl_2 optical techniques can be used with specimens which have quite well defined demagnetizing factors, e.g., small areas at the center of thin sheets with large width to thickness ratios. Finally, we note that rotation measurements and closely related birefringence measurements are widely applicable to the study of magnetic and structural phase transitions.

A complex magneto-optical rotation in paramagnetic substances may be thought of as arising from the sum of contributions from optical transitions which are allowed for positive and negative circularly polarized radiation. Note that FeCl_2 is

optically uniaxial. Strictly speaking the normal modes of propagation are circular only for light traveling along the principal axis, and only in that case is the following decomposition valid. In our experiments, great care is taken to have the field perpendicular to the basal plane and to use a narrow cone of light coaxial with the optical and crystalline axes. If linearly polarized light enters the crystal under these conditions, the emergent light may be elliptically polarized. The real part of the magneto-optical rotation corresponds to the rotation of the major axis relative to that of the incident light. The imaginary part gives the ellipticity of the emergent light. The two quantities are obviously closely related, but we fix our attention on the rotation in spectral regions where the crystal is quite transparent, and ellipticity is very small.

Equation (1) expresses the rotation arising from transitions between a Boltzmann occupied set of ground states a and excited states b :

$$\Phi = K \frac{(\langle n \rangle + 2)^2}{\langle n \rangle} \sum_{a,b} \frac{\omega^2 / \omega_{ba}}{(\omega_{ba}^2 - \omega^2)} (f_{ba}^+ - f_{ba}^-) \rho_a^0. \quad (1)$$

This is a simplified form of a general equation given by Shen.¹¹ It omits damping terms and thus pertains to spectral regions where there is rotation, but little absorption. In it, $K = \pi e^2 N / 9mc$, $\langle n \rangle$ is the average refractive index, f_{ab}^\pm are the oscillator strengths for the two circular waves, and ρ_a^0 contains the Boltzmann populations of the unperturbed ground states. This equation applies to a situation in which there are levels a of a ground state variously occupied. These are connected by electric dipole transitions to excited states b . The contribution of each transition is determined by the population of a and the strength of the transition. Note that the average refractive index enters the prefactor to modify the summations slightly. Each transition makes a dispersive contribution to the total rotation.

We present in Fig. 3 measurements of the magneto-optical rotation of FeCl_2 as it varies with photon energy from the near infrared to a band edge at which our specimen becomes opaque. These were made with the crystal nearly saturated in the paramagnetic state at 4.2 K in a field of 19 kOe. The specimen was 90 μm thick, but note that we quote specific rotation. If the prefactor in Eq. (1) is constant, only one transition is operative, and the damping terms are negligible, we would expect rotation

$$\Phi = K' \{ (\hbar\omega)^2 / [(\hbar\omega_{ab})^2 - (\hbar\omega)^2] \}. \quad (2)$$

We find that quite a reasonable fit can be achieved with $K' = 5.0 \times 10^2$ deg/cm and $\hbar\omega_{ab} = 3.3 \times 10^4$ cm^{-1} . This curve is plotted as the solid line. We inter-

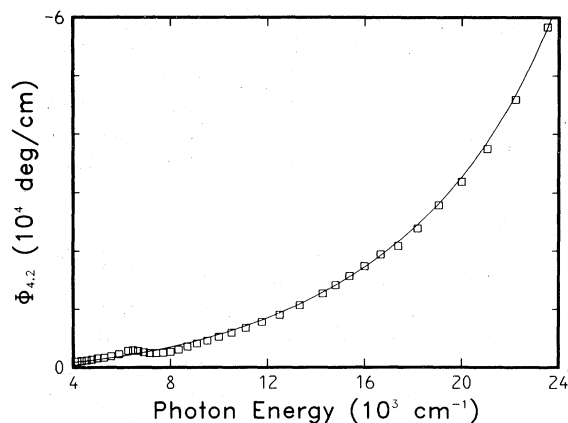


FIG. 3. Points represent the specific magneto-optical rotation of FeCl_2 at 4.2 K with $H_a = 19$ kOe. Both field and light propagation direction are parallel to [0001]. The solid curve is $\Phi = (508. \text{ deg/cm})(\hbar\omega)^2/[(\hbar\omega)^2 - (33\,023 \text{ cm}^{-1})^2]$.

pret this as indicating that transitions at about $33\,000 \text{ cm}^{-1}$ are responsible for the rotations used here to study the phase diagram of FeCl_2 . The small dispersive anomaly near 7000 cm^{-1} is an example of another term in the summation. It is associated with an absorption peak at about $1.45 \mu\text{m}$ in the data of Schnatterly *et al.*¹² This is attributed to the first crystal-field transition ${}^5T_2 - {}^5E$.

We return now to the relation between $\Phi(T, H)$ and $M(T, H)$. From (1) it may be seen that the optical rotation in FeCl_2 is approximately proportional to the difference in the population of the $m = \pm 1$ states of the lowest-energy spin-orbit triplet. (The rotation vanishes if time-reversed states are equally populated.) This population difference is just the magnetization. Thus, Φ and M are approximately proportional. The proportionality is not exact, however, because of small variations of the oscillator strengths, the excitation frequencies and the average refraction index with H and T .

We would like to estimate the error which we might make in assuming that Φ and M are directly proportional. To do this, we *define* a proportionality factor by¹³

$$A(H, T) = \Phi(H, T)/M(H, T). \quad (3)$$

If Φ and M were truly proportional, A would be independent of H and T . In reality $A(H, T)$ is not constant. Indeed, like all properties of the system it should have a component which is singular at the phase transitions. Nonetheless, we believe that the variation of A is negligible for our purposes. We have two experimental checks of this. The first check is indirect. We note that the

various factors in (1) which might change A , also directly affect the average refractive index. We have a measure of the variation of the average refractive index through the polarization dependence of the light scattering by the mixed phase.¹⁴ The results show a maximum change of about one part in 2000. This is enough to cause significant effects in the light scattering, but is quite negligible for the interpretation of the phase diagram.

A more direct test of the constancy of A is obtained from the slope of $\Phi(H_{\text{ext}})$ in the mixed phase region. The external field for T fixed, varies directly with M , the proportionality constant being the demagnetizing factor. Thus the variation in the slope measures the variation in A . From our data, the slope varies by less than one part in 130 along the whole length of the first-order boundary from 4.2 to about 21. Thus, it appears that $\Phi(T, H)$ is closely proportional to $M(T, H)$ over the fields and temperatures of interest to us.

IV. ROTATION MEASUREMENT

During the course of this work, our experimental techniques have evolved so that two methods have been used to collect rotation data. In both cases a rotating analyzer produces a signal, and a minicomputer is used in the collection, manipulation, and storage of the data. Our use of a rotating analyzer has been described before.¹⁵ Briefly, linearly polarized monochromatic light is transmitted by a thermostatted specimen in a field which lies along the axis of the optical system. The beam having thus undergone a rotation encounters first a linear analyzer rotating with angular velocity $\frac{1}{2}\omega$ and then a detector. The rotation is contained in the phase of the $\cos\omega t$ signal seen at the detector. A large part of our data were obtained by using a commercial phase computer to produce a voltage proportional to the phase angle between the detector signal and a reference obtained from the rotating analyzer itself. The magnetic field is represented by the voltage of a Hall probe taped to one of the pole pieces. As the field is varied slowly, data pairs, voltages representing field and rotation, are digitized and stored in the computer memory. The characteristics of the phase computer limit the angular resolution to about 0.15° .

More recently the rotation has been measured by an inherently computer-based technique which is capable of much greater resolution. As above, the rotating analyzer produces a sinusoidal detector signal. Following the techniques of Aspnes,¹⁶ the photomultiplier output is sampled and digitized 18 times in one cycle of the output voltage. These

values are added in the correct sequence to the (initially zero) contents of 18 memory locations. The process is repeated hundreds or thousands of times, then terminated. The contents of the 18 locations are then Fourier analyzed to yield the phase of the detector signal, the magneto-optical rotation. Meanwhile the field is stepped to a new value, and the process repeated. Field-rotation pairs are stored in a data array. The analyzer rotates at about 53.5 Hz, so the signal is at 107 Hz. One hundred readings of the photomultiplier voltage require only 1 sec, and these yield values of rotation good to 0.01° . Four hundred readings require about 4 sec, and yield values of rotation good to about 0.005° .

In both cases the numerical arrays of data may be manipulated in various ways. The raw field voltages may be subjected to calibrations and converted to a corrected field. Rotation can be reduced by dividing by the 4.2-K value.

We will henceforth indicate reduced rotation by $\phi = \Phi(T, H)/\Phi(4.2 \text{ K}, 19 \text{ kOe})$. Field may be replaced by internal field. The whole array or any part of it can be displayed on a cathode-ray-tube (CRT) screen and special points read from the screen with a cursor. The data array or any of its progeny can be readily stored on magnetic cassettes and worked on at some later time.

V. LIGHT SCATTERING

Coexisting mixtures of antiferromagnetic and paramagnetic material at the first-order metamagnetic transition of FeCl_2 have been found to scatter light.¹⁴ As detailed in a recent study, the scattering appears abruptly on entering the mixed phase region, and thus is useful in measuring the boundaries of the mixed phase in the applied field temperature plane. The scattering peaks somewhere in the middle of the mixed phase region at any temperature. The effect decreases as temperature increases and the tricritical point is approached. It increases with decreasing wavelength. The fact that in FeCl_2 the scattering is markedly greater for one circular polarization than for the other was a considerable surprise, and is dealt with in Ref. 14. Griffin *et al.*¹⁷ encountered this polarization-dependent scattering as an apparent circular dichroism, and in their early work used that quantity to plot the edges of the mixed phase. On the antiferromagnetic phase boundary they found it useful to within about 1 K of the tricritical point. Recently Giordano¹⁸ and Giordano and Wolf¹⁹ have reported the use of scattering techniques to study the tricritical behavior of dysprosium aluminum garnet. Wood and Day²⁰ used them to follow the evolution of the

magnetic phase diagram of $\text{Fe}_p\text{Mg}_{1-p}\text{Cl}_2$ as ρ approached the percolation limit of about 0.6.

In these experiments the scattering was measured at fixed temperature for various values of applied field. Monochromatic light, typically $\lambda = 0.7 \mu\text{m}$, was exactly circularly polarized with a Glan Thomson prism and a Babinet Soleil compensator. Naturally, the compensator was set to produce the more strongly scattered polarization. This passed through the sample, was chopped at 400 Hz and detected using a photomultiplier and a phase sensitive detector. The output of the phase sensitive detector was digitized along with a Hall voltage representing the applied field. The usual procedure was to repeat the experiment 64 times, and to add the digits representing intensity in each small field interval at a specific memory location. At the end of the data accumulation phase each of these was divided by the number of readings in the sum. This multichannel analyzer mode of data collection gave plots of transmitted intensity versus field on which the scattering could be clearly defined to within about 0.02 K of the tricritical point. The scattering data array at this point consisted of intensity-field pairs. This was read by displaying the whole array at an appropriate scale on the cathode-ray screen of a Tektronix 4010-1 terminal, intensity vertical, field horizontal. The array of points designated (a) on Fig. 4 serves as an example. The pronounced dip between the arrows indicates the decrease in transmitted intensity due to scattering. On the same screen we would also display the rotation-

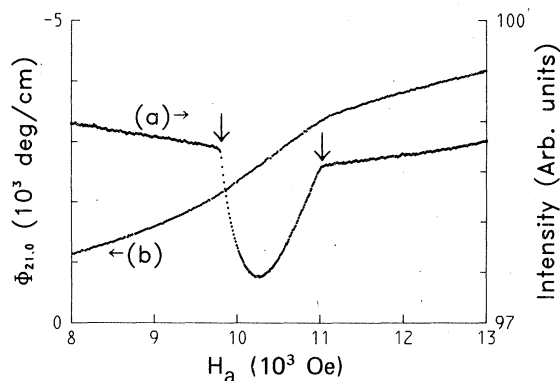


FIG. 4. Computer display of scattering and rotation data points as a function of applied field for 21.2 K. The array of points (a) are the scattering data. The pronounced dip in intensity between the arrow marked points is due to scattering out of the beam by the mixed phase. The array (b) constitute the rotation versus field measurements. The technique used to read the coordinates of the phase boundary is described in the text. Note that the scattering data represent the average of 64 field sweeps.

field array made at the same temperature. On Fig. 4 these points are marked (b). The mixed phase corresponds to a straight segment of this curve. However, the gradual approach to this straight line makes it very difficult to define the phase boundaries. Our technique is to set a vertical cursor at the field of the last point in (a) which does not deviate from the smooth curve. The point at which this crosses the array (b) is used to set the horizontal cursor. The computer then is directed to read the setting of the two cursors. For the temperature at which the two sets of data were acquired, we have values for H_a and ϕ . The procedure is then repeated for the high-field point. Phase diagram coordinates are thus contained in these sets of values, temperature, applied field, and reduced rotation.

Section IV contained a description of the techniques used to read the coordinates of the phase boundaries from combined scattering and rotation data. These are useful in the high interest region just below the TCP. For some fields and temperatures other procedures are appropriate. For instance, at low temperatures the breaks in the $\phi(H_a)|_T$ are sufficiently sharp so that it is not necessary to invoke the scattering technique. T , H_a , and ϕ can be read directly from the plots of the data arrays.

In principle, points along the λ line could be ob-

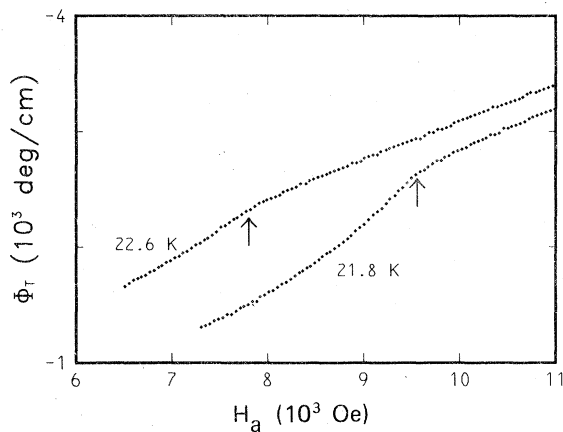


FIG. 5. Plots of $\Phi(H_a)$ arrays at 21.8 and 22.6 K. The wavelength was $0.8 \mu\text{m}$. The rotations shown have been corrected for the incidental rotations of lenses and windows in the magnetic field. They can be converted to relative rotation ϕ by dividing by 67.64° , the 4.2-K rotation for the paramagnetic state. Raw Hall voltages have been subjected to a calibration to provide the field values plotted. Arrows are used to indicate the points we have taken to be the crossings of the λ line. The 22.6-K points have been shifted upward by $0.2 \times 10^3 \text{ deg/cm}$ for clarity. Similarly, half the points in each array have been omitted. These data were taken with a commercial phase computer.

tained from the location of discontinuities on $\phi(H_a)|_T$ or $\phi(T)|_{H_a}$ plots. Figures 5 and 6 each give two examples of these plots. Along the whole length of the λ line and especially toward the high-temperature end, the $\phi(T)|_{H_a}$ curve crosses the second-order boundary much more steeply than the $\phi(H)|_T$ curve; consequently the discontinuity is inherently easier to read on the $\phi(T)|_{H_a}$ plots. In reading the coordinates of the point at which the λ line crosses both of these curves, our criterion with both plots is to take the last point before the slope of the rotation starts to decrease. We have marked the value read from the various curves in the two figures.

VI. PHASE DIAGRAMS

Using the techniques just described we have assembled an array of T , H_a , ϕ points which appear to lie on phase boundaries. In the temperature interval from 4.2 to 20.9 K, 42 pairs of points, one on the upper boundary, one on the lower, were obtained by locating discontinuities on $\phi(H)|_T$ curves. Fifty-eight points along the upper branch (above 18.85 K) and the λ line were obtained from the discontinuity in the $\phi(T)|_H$ curves. Finally in the region of highest interest just below the tricritical point 13 pairs of points were extracted from scattering and rotation data by the technique illustrated in Fig. 4. These range in temperature from 21.00 to 21.50 K.

The phase diagrams given by this total array are presented in three figures, the H_a - T plane in Fig. 7, the ϕ - T plane in Fig. 8, and the H_i - T plane in Fig. 9. The overall aspect of these three diagrams is closely parallel to the established pic-

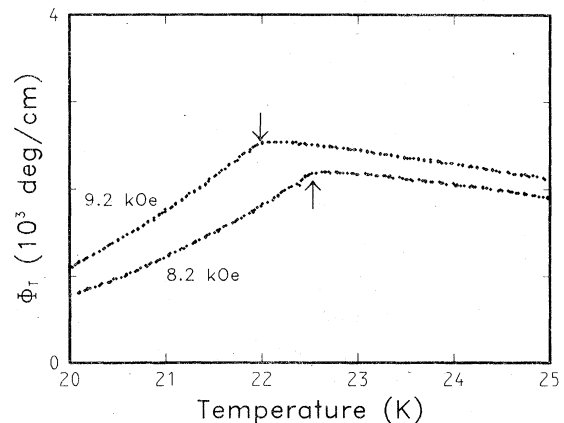


FIG. 6. Plots of $R(T)$ data arrays at 8.2 and 9.3 kOe. The wavelength was $0.8 \mu\text{m}$. The rotations have been corrected and can be converted as in Fig. 5. Again arrows are used to indicate the points we take as the crossing of the λ line. For clarity half the points in each array have been omitted.

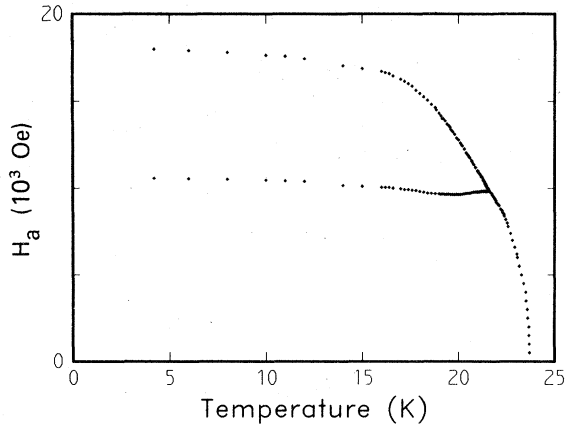


FIG. 7. Magnetic phase diagram of FeCl_2 in the H_a - T plane. Fields are along [0001], and the diagram applies to a very thin (0001) sheet.

ture of FeCl_2 , though there is a considerable variation in the values of T_N and T_t reported by different groups and listed in Table I. Later we will discuss our values for these temperatures. As will be developed below, we believe that on re-interpretation the Birgeneau *et al.* values will coincide with ours; further, that the discrepancies with the Griffen and Schnatterly and with the Vet-

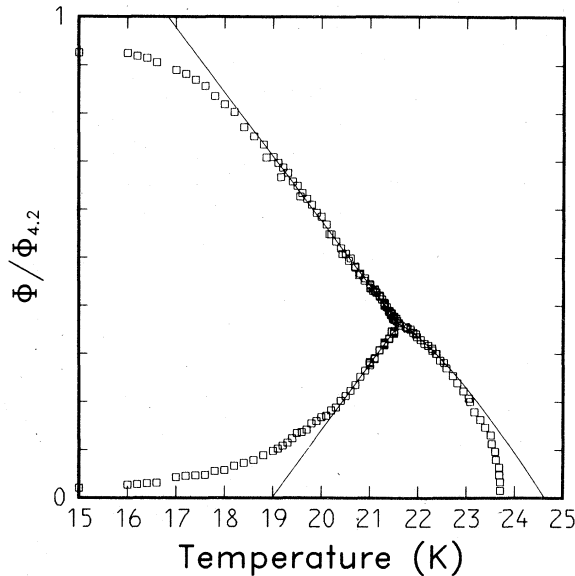


FIG. 8. The high-temperature end of the magnetic phase diagram of FeCl_2 in the ϕ - T plane. ϕ is the reduced magneto-optical rotation, i.e., the measured rotation divided by the rotation for the same sample at the paramagnetic state at 4.2 K. Magnetic field and light propagation direction are along [0001]. The solid lines represent the fit we have made to these data to obtain the coordinates of the tricritical point and the exponents describing the approach. Detailed ranges and parameters are given in Table II.

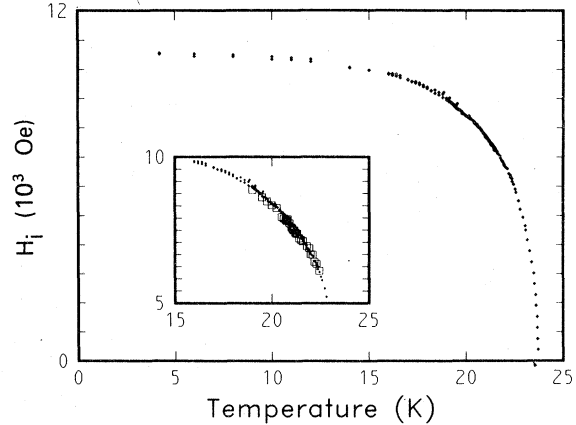


FIG. 9. Magnetic phase diagram of FeCl_2 in the H_i - T plane. This applies to fields along [0001]. Insert shows the points from Ref. 5 plotted on top of ours without adjustment.

tier values may represent a difference in sample composition or in thermometry, as well as somewhat less accurate determinations than reported here.

The ϕ - T diagram of Fig. 8 corresponds closely to an M - T diagram. Following the discussion in Sec. III, we cautiously regard it as equivalent. Note that $H_i = H_{\text{ext}} - NM = H_{\text{ext}} - N\phi/A$. From this it is clear that the constant slope of $d\phi/dH_{\text{ext}}$ at various temperatures across the mixed phase region constitutes a measure of the (demagnetizing factor N)/(proportionality constant A). Furthermore, it is in the correct units to convert $\phi(H_{\text{ext}})$ to $\phi(H_i)$. From the dimensions of the sample (a thin sheet with axial ratio of about 50:1) it is clear that N is within a few percent of 4π . Using the averaged N/A , we can transform the T, ϕ, H_a array to T, ϕ, H_i .

From these points the H_i - T plane phase diagram of Fig. 9 has been plotted. The upper and lower branches collapse onto a single line, and the resultant curve goes smoothly through the tricritical point marked with an arrow.

VII. TRICRITICAL POINT AND ITS APPROACHES

Points on the M - T diagram near the intersection of the first-order lines and the λ line were used to determine the tricritical point as well as the slopes and exponents describing the approaches to it. The fitting was done using a multiparameter nonlinear least-squares fitting program. Several steps were involved, so that the decision as to which branch points close to the tricritical point belonged was not made until its location was determined quite closely. The system of equations we have fitted is

TABLE I. Tricritical and Néel temperatures of FeCl₂.

Author	T_t	T_N	T_t/T_N
Vettier ^a	20.3	22.9	0.886
Griffin ^b	20.79	23.0	0.904
Birgeneau ^c	21.15	23.6	0.896
Present work	21.60	23.7	0.911

^aC. Vettier, thesis (Grenoble, 1975).

^bReported in Ref. 5.

^cReported in Ref. 4.

for the upper branch,

$$\phi = \phi_t + B_+(1 - T/T_t)^{\beta_+},$$

for the lower branch,

$$\phi = \phi_t - B_-(1 - T/T_t)^{\beta_-},$$

and for the lambda line,

$$\phi = \phi_t - B_\lambda(T/T_t - 1)^{\omega_\lambda}.$$

Eight parameters were simultaneously fitted, the coordinates T_t and ϕ_t of the tricritical point, the factors B_+ , B_- , and B_λ as well as β_+ , β_- , and ω_λ , the exponents describing the curvature of these approach lines. A decision must be made as to which points to include, and this is essentially empirical. We find that the tricritical point is not very sensitive to this choice, but the other parameters are. Bearing in mind the theoretical expectation of linear approaches on the low field side, we see in Fig. 8 that the points of the paramagnetic branch fall closely on a straight line down to about 19 K, then diverge. A similar examination has led us to include points within different ranges along each branch for the final fitting. For the paramagnetic line points within $19 \text{ K} \leq T \leq T_+$ were used; for the antiferromagnetic line $20.5 \text{ K} \leq T \leq T_t$; for the λ line, $T \leq T \leq 22.3 \text{ K}$. The final parameters are given in Table II along with those reported by previous workers. Inclusion of points beyond these ranges would introduce curvature, use of shorter ranges would give similar parameters with greater and greater errors.

The solid lines in Fig. 8 correspond to the parameter values given in Table II. The range over which points on the first-order lines are linear seems clearly to reflect asymptotic behavior. On the λ line it is less clear, and the small number of points leads to rather large errors in ω_λ and B_λ . The first-order phase boundaries are consistent with the theoretical expectation of linear approaches to the TCP. We interpret the different ranges as reflecting the extent of the tricritical region. Figure 10 shows log-log plots of the three branches as they approach the TCP. Table II also

TABLE II. Tricritical point and exponents.

Quantity	Birgeneau ^a	Griffin ^b	Present work ^c
T_t	21.15	20.79 ± 0.11	21.60 ± 0.02 K
m_t, ϕ_t	0.395	0.38 ± 0.01	0.361 ± 0.002
β_+	≈ 1	1.03 ± 0.05	1.00 ± 0.02
β_-	0.36	1.13 ± 0.14	1.00 ± 0.07
β_μ	d	1.1 ± 0.11	1.00 ± 0.08
ω_λ	≈ 1	d	1.29 ± 0.16
B_+	d	2.85 ± 0.34	2.89 ± 0.10
B_-	d	4.14 ± 1.5	3.0 ± 0.6
B_λ	d	d	4.6 ± 2.6
$\frac{dm_+}{dt}$	d	2.66 ± 0.11	2.8 ± 0.1 ^c
$\frac{dm_\lambda}{dt}$	d	1.57 ± 0.08	1.57 ± 0.1 ^e

^a Values published in Ref. 4.

^b Values published in Ref. 5. Those for B_+B_- and the slopes of m_+ and m_λ were normalized to $M_{4,2}$ to match our usage.

^c Obtained by least-squares fit to 100 points in range: $19 \leq T \leq T_t$ along the paramagnetic branch; $20.5 \leq T \leq T_t$ along the antiferromagnetic branch; $T_t \leq T \leq 22.3$ along the λ line. In reduced temperature the data along the paramagnetic line are in $0.002 \leq t \leq 0.12$, the antiferromagnetic in $0.0046 \leq t \leq 0.05$, and the λ line in $0.0014 \leq t \leq 0.03$.

^d Values not given in the reference cited.

^e Read graphically from Fig. 11.

includes a value for the exponent β_μ describing the disappearance of $\phi_+ - \phi_-$ on approaching the TCP. The pertinent equation is

$$\phi_+ - \phi_- = B(1 - T/T_t)^{\beta_\mu}. \quad (4)$$

An important result of renormalization-group theory is that, for tricritical points, classical mean-field theory is valid down to dimension three rather than dimension four as in the case of ordinary critical points. However, at the critical dimension three the theory predicts logarithmic corrections to the classical exponential approaches the tricritical points but there is no indication of the size of these terms. Thus, it is desirable to see whether the present data are better fitted by expressions with logarithmic corrections than by simple exponentials. In another case where three is the marginal dimension, that of the uniaxial dipolar coupled ferromagnet LiTbF₄, Giffin, Litster, and Linz²¹ recently showed that an expression with a logarithmic correction gave a better fit to the data than the usual exponential relation.

Stephen, Abrahams, and Straley²² and later

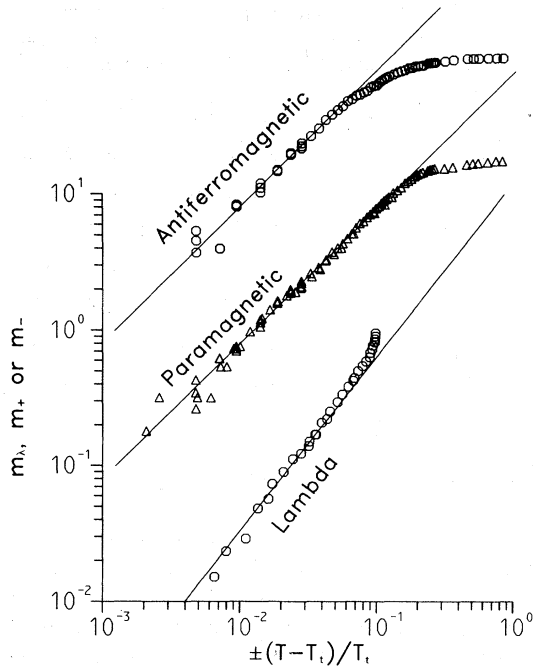


FIG. 10. Log-log plots of the reduced magnetization against reduced temperature for data points on the three branches as they approach the tricritical point. For clarity, the points along the paramagnetic branch have been displaced upwards one decade, those along the antiferromagnetic branch two decades.

Giordano¹⁸ have given expressions for the approach of the paramagnetic and antiferromagnetic lines to the tricritical point. We have tried to fit our data on these two branches over several ranges of reduced temperature to these expressions. In no case did this give a fit which was better than that of the corresponding exponential fit based on fewer adjustable parameters. Goodness of fit was judged by the sum of the squares of the deviations. The errors in the parameters pertaining to the logarithmic correction were larger than the resultant parameters themselves. That such corrections would fail to improve on our exponential fit is not surprising since β_+ and β_- both came out very close to 1.000. The logarithmic terms are corrections to a term linear in t .

VIII. DISCUSSION

In addition to providing more accurate data on the FeCl₂ TCP, we hoped that these experiments would clarify the discrepancy between the results of Birgeneau *et al.*⁵ (BSBK) on one hand and those of Griffin and Schnatterly⁶ (GS) on the other. That discrepancy primarily concerns the approach of the lower first-order branch to the TCP, and shows up in the values of β_- in Table II. Griffin

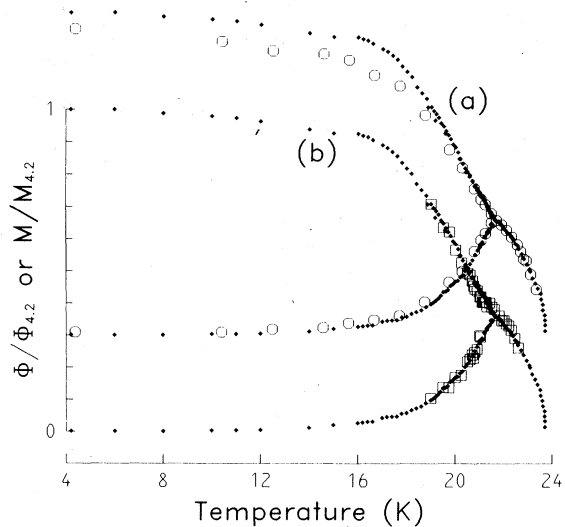


FIG. 11. Attempted superpositions of earlier data on the present data over the whole temperature range. (a) Griffin and Schnatterly data (open octagons) scaled so as to best coincide with ours (solid diamonds) around the TCP. These have been displaced upward by 0.3. (b) Birgeneau *et al.* data (open squares) scaled very slightly to coincide with ours near the TCP.

and Schnatterly reported a value of 1.13 ± 0.14 , a nearly linear approach, whereas Birgeneau *et al.* reported 0.36. To illuminate the differences among the three sets of data we attempted to superimpose them using a simple procedure. For each of the three sets, M - T plots were made for the range 18–23 K. By superimposing these in the neighborhood of the TCP, we readily determined the factors by which both temperature and reduced magnetization coordinates of the two earlier sets must be multiplied in order to best coincide with our data. Using these correction factors the GS and BSBK data were separately plotted with our data. Figure 11 (a) shows the GS data and our data over the full temperature range, while Fig. 12 (a) is an expanded plot around the TCP. The necessary scaling has multiplied the GS temperatures by 1.041 and magnetizations by 0.95. The approaches to the TCP are very similar, though there is obviously a systematic discrepancy along the paramagnetic line where the GS points all lie below ours. It seems likely that these differences arise from the differing relationships between M and $1.4 \mu\text{m}$ magnetic circular dichroism in the GS case and M and magneto-optical rotation in our experiments. This difference also appears in the values of M_t given in Table II. It seems possible that the temperature discrepancy of about 0.8 K in T_t and T_N arises from a composition difference or perhaps in part from a difference in thermometer calibration.

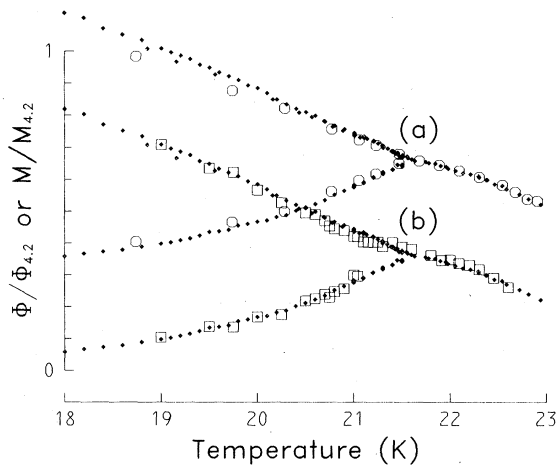


FIG. 12. Attempted superpositions of earlier data on the present data near the TCP. (a) Griffin and Schnatterly data (open octagons) scaled so as to best coincide with ours (solid diamonds) around the TCP. For clarity these have been displaced upward by 0.3. (b) Birgeneau *et al.* data (open squares) scaled very slightly to coincide with ours near the TCP.

A parallel comparison is made between the BSBK data and ours in Figs. 11(b) and 12(b). Here again we have attempted an overall superposition of the phase boundaries as they approach the TCP. The requisite scaling only shifted T infinitesimally and M by a factor of 1.02. With such a shift the three phase boundaries coincide extraordinarily well except for the immediate region of the intersection. Relative to our data, the points along the lower first-order branch are missing in the BSBK data, a region in which our data show six consistent points, and the GS data show two points. Parenthetically we note that if the TCP's are made to coincide, rather than the phase boundaries as above, the antiferromagnetic lines would be very far apart. Figure 12(b) achieved almost without adjustment, is compellingly plausible superposition.

An outstanding feature of the comparisons made

above is the absolute agreement between the M - T phase diagram points obtained by our optical techniques and those obtained by BSBK with neutron-diffraction techniques. In hindsight, it is clear that the nature of the diffraction experiments precluded the determination of points along the antiferromagnetic line above 21.1 K. Without these it was not possible to determine the TCP, and the authors turned to an alternate criterion based on critical scattering.²³ This yielded a value for T_t a half-degree lower than the value we now take to be correct. The remarkable agreement of the phase boundary data forces us to conclude that the criterion used, though exceedingly reasonable, is subject to some ambiguity.

Our final view is that the present data, a slight scaling of the GS data and the BSBK phase boundary points are all in substantial agreement with each other. The exponents obtained will all describe nearly linear approaches to the TCP. Thus data from radically different experiments all accord with tricritical theory. Not only have different techniques been used, but the neutron-diffraction experiments measure the antiferromagnetic order parameter M_s whereas all the optical techniques measure the other order parameter in the problem M . In order to provide a test of the scaling hypothesis for FeCl_2 , further careful measurements of $\phi(T, H_4)$ in the neighborhood of the TCP are in progress. They will be reported in a later publication.

ACKNOWLEDGMENTS

The authors wish to express very special thanks to R. J. Birgeneau for an introduction to FeCl_2 and for many illuminating discussions in the course of this work. We are pleased to acknowledge with thanks R. Alben's consideration of the relations of rotation to magnetization. We thank N. Giordano and W. P. Wolf for a series of profitable discussions and P. Hohenberg for a discussion of logarithmic corrections.

¹R. J. Birgeneau, W. B. Yelon, E. Cohen, and J. Makovsky, *Phys. Rev. B* **5**, 2607 (1972); R. Alben, *J. Phys. Soc. Jpn.* **26**, 261 (1969).

²R. Bausch, *Z. Phys.* **254**, 81 (1972).

³See, for example, G. Goellner and H. Meyer, *Phys. Rev. Lett.* **26**, 1534 (1971).

⁴H. Giordano and W. P. Wolf, *Phys. Rev. Lett.* **35**, 799 (1975).

⁵R. J. Birgeneau, G. Shirane, M. Blume, and W. C. Koehler, *Phys. Rev. Lett.* **33**, 1098 (1974); R. J. Birgeneau, *AIP Conf. Proc.* **24**, 258 (1974).

⁶J. A. Griffin and S. E. Schnatterly, *Phys. Rev. Lett.*

33, 1576 (1974); J. A. Griffin and S. E. Schnatterly, *AIP Conf. Proc.* **24**, 195 (1974). J. A. Griffin, Ph.D. thesis (Princeton University, 1974) (unpublished).

⁷W. P. Wolf, *Physica (Utr.) B* **86-88**, 550 (1977).

⁸E. Yi Chen, J. F. Dillon, Jr., and H. J. Guggenheim, *AIP Conf. Proc.* **18**, 329 (1973).

⁹Liquid Transfer Heli-tran Refrigerator, Air Products and Chemicals, Inc.

¹⁰Cryogenic Capacitor Controller, Lake Shore Cryotronics, Inc.

¹¹Y. R. Shen, *Phys. Rev. A* **133**, 511 (1964).

¹²S. E. Schnatterly and M. Fontana, *J. Phys.* **33**, 691

- (1972).
- ¹³R. Alben (private communication).
- ¹⁴J. F. Dillon, Jr., E. Yi Chen, H. J. Guggenheim, and R. Alben, Phys. Rev. B 15, 1422 (1977).
- ¹⁵J. F. Dillon, Jr., E. Yi Chen, and H. J. Guggenheim, AIP Conf. Proc. 24, 200 (1974).
- ¹⁶D. E. Aspnes and A. A. Studna, Appl. Opt. 14, 220 (1975).
- ¹⁷J. A. Griffin, S. E. Schnatterly, Y. Farge, M. Regis, and M. P. Fontana, Phys. Rev. B 10, 1960 (1974).
- ¹⁸N. Giordano, Ph.D. thesis (Yale University, 1977) (unpublished).
- ¹⁹N. Giordano and W. P. Wolf, Phys. Rev. Lett. 39, 342 (1977); Physica (Utr.) B 86-88, 593 (1977).
- ²⁰T. E. Wood and P. Day, J. Phys. C 10, L333 (1977).
- ²¹J. A. Griffin, J. D. Litster, and A. Linz, Phys. Rev. Lett. 38, 251 (1977).
- ²²M. J. Stephen, E. Abrahams, and J. P. Straley, Phys. Rev. B 12, 256 (1975).
- ²³R. J. Birgeneau (private communication).